Anomaly in the transverse longitudinal ratio for $^3He(e,e'p)X$ reaction at 260 MeV/c recoil momentum

J. M. Le Goff,[1] M. Bernheim,[1] M. K. Brussel,[2] G. P. Capitani,[3] J. F. Danel,[1] E. De Sanctis,[3] S. Frullani,[4] F. Garibaldi,[4] F. Ghio,[4] M. Jodice,[4] A. Magnon,[1] C. Marchand,[1] Z. E. Meziani,[5,*] J. Morgenstern,[1] P. Vernin,[1] and A. Zghiche[1,†]

[1]*Service de Physique Nucléaire (SPhN) CEA Saclay, F-91191 Gif-sur-Yvette Cedex, France*

[2]*Department of Physics, University of Illinois at Urbana Champaign, Urbana, Illinois 61801*

[3]*Laboratori Nazionali di Frascati, Istituto Nazionale di Fisica Nucleare, I-00044 Frascati, Italy*

[4]*Laboratori di Fisica, Istituto Superiore di Sanitá and Istituto Nazionale di Fisica Nucleare, Sezione Sanitá I-00161 Roma, Italy*

[5]*Department of Physics, Stanford University, Stanford, California 94305*

(Received 10 September 1996; revised manuscript received 15 November 1996)

$^3He(e,e'p)X$ cross sections were measured in parallel kinematics for recoil momenta around 260 MeV/c. A Rosenbluth decomposition of the cross section was made and transverse and longitudinal spectral functions were extracted. The longitudinal spectral function is strongly quenched relative to the transverse one, the ratio of the integral of the longitudinal to transverse spectral functions over the continuum channel being $0.175\pm0.046\pm0.049$. A model which takes into account final state interactions and meson exchange currents predicts a ratio of 0.43, it can therefore explain only part ot the quenching. [S0556-2813(97)04602-5]

PACS number(s): 21.45.+v, 21.30.Cb, 25.30.Fj

We present the results of a study of high proton momenta in ^3He, as measured through the $(e,e'p)$ reaction. The transverse and longitudinal components of the cross section were determined separately; this paper is therefore complementary to [1] where no separation was performed.

Despite the success of the independent particle shell model, we know that the nucleus cannot be fully described in terms of one-body properties. A considerable theoretical effort has been made to encompass two-body properties in the description. However, as described in [1], aside from measurements [1,2] of high proton momenta via the $(e,e'p)$ reaction [3], little experimental information is available on two-body properties and what does exist is rather indirect.

Measurements of high proton momenta can indeed yield information about two-body properties, since the highest momentum components of the nuclear wave function are generated by nucleon-nucleon correlations [4]. It has been predicted [5,6] that for high recoil momenta in the $(e,e'p)$ continuum channel, i.e., when the recoil system is unbound, the cross section is dominated by the process illustrated by Fig. 1: the electron scatters quasielastically from a proton belonging to a close together nucleon pair, the second nucleon of this pair carrying off most of the recoil momentum, p_r. The residual nuclear system is assumed to remain a ''spectator'' and is practically at rest. In their center of mass, due to their proximity, the two nucleons of the pair have large equal and opposite momenta. In this picture, the recoil system consisting of the second nucleon of the pair plus the $A-2$ spectator nucleons of mass M_{A-2} has a mass

$$M_r^2=[M_{A-2}+\sqrt{M_n^2+p_r^2}]^2-p_r^2. \qquad (1)$$

When the relative momentum of the pair and the spectator $A-2$ system is considered, M_r is no longer completely fixed but can vary around the value above. A signature of this process can be defined by displaying the cross section as a function of the missing energy, $E_m=M_p+M_r-M_A$ (M_p and M_A are the proton and the target masses): a peak is expected, whose position shifts predictably with increasing recoil momentum, i.e., according to Eq. (1). The momentum distribution in the continuum at high p_r is then the momentum distribution of a proton in a pair of nucleons close together. The width of the peak reflects the momentum of the pair in the target nucleus.

This picture was successfully tested in the relatively loosely bound ^3He nucleus [2], and then in the more tightly bound and dense ^4He nucleus [1]. The peak was observed as expected. Moreover, the proton momentum distributions in the continuum of ^3He and ^4He were extracted from the data

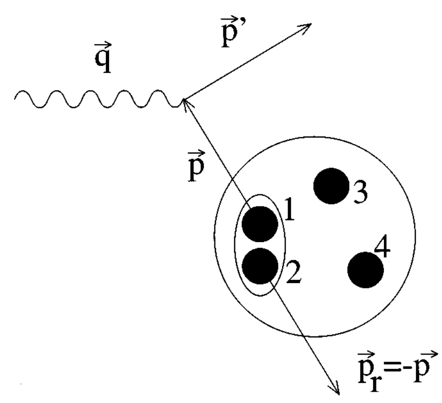

FIG. 1. The virtual photon is absorbed by nucleon (1), the nearby nucleons of the pair (1+2) have large equal and opposite momentum, p. The $A-2$ other nucleons (here 3 and 4) are spectators and have no net momentum, nucleon (2) carries off all the recoil momentum.

*Present address: Temple University, Philadelphia, PA 19122.

†Present address: Centre de Recherches Nucléaires, 67037 Strasbourg, Cedex, France.

and found, for $p_r > 100$ MeV/c, to be quite similar to that of deuterium, i.e., of an n-p pair which is not embedded in a nuclear medium. The relative momentum distribution of two close nucleons inside a nucleus thus appears to be only slightly affected by the nuclear medium.

With a moderate energy accelerator (700 MeV), such experiments can only be performed in the so called ''dip'' region [7], which in an inclusive (e,e') spectrum lies between the quasielastic peak and the delta region. This is a region where complicating reaction mechanisms, especially meson exchange current (MEC's), can be important. Such effects have been predicted to affect the cross section only at the 20% level [8]. However, theory is often unsuccessful in reproducing the inclusive (e,e') cross section in this ''dip'' region. In order to estimate the importance of reaction mechanism effects and to test theoretical calculations of them, we have performed a Rosenbluth transverse longitudinal (T/L) separation of the $^3\mathrm{He}(e,e'p)X$ cross section in the ''dip'' region at relatively high recoil momentum. Since the transverse (T) and longitudinal (L) components correspond to different couplings, magnetic and Coulomb, respectively, the requirement that the calculations reproduce both simultaneously provides a stringent test of our understanding of the reaction mechanism. Furthermore, the longitudinal component, which couples directly to the charge, is expected to be less sensitive to MEC's, which happen to have a large contributions in the dip region.

In this paper we follow the notation of Ref. [9] and we present results for both the continuum channel, where the recoil is unbound $(X=pn)$, and the two-body break up $(2bbu)$ where the recoil is bound $(X={}^2\mathrm{H})$. For ''parallel'' kinematics, i.e., when the ejected proton momentum $\mathbf{p}'$ is parallel to the momentum transfer $\mathbf{q}$, the $(e,e'p)$ cross section can be written $\sigma=\Gamma(T+\epsilon L)$, where Γ is the flux of virtual photons with longitudinal polarization ϵ. From the measured T and L one can then define ''experimental spectral function,''[1] $S_T^{\mathrm{expt}}=T^{\mathrm{expt}}/T^p$ and $S_L^{\mathrm{expt}}=L^{\mathrm{expt}}/L^p$. In the present analysis, T^p and L^p are derived from the De Forest [10] off-shell electron-proton cross section denoted as ''cc1.'' In the simplest approximation [plane-wave impulse approximation (PWIA)] the two spectral functions are equal and represent the probability to find inside the target nucleus a proton with momentum P_r and binding energy E_m. A T/L separation requires two measurements with different electron scattering angle $\theta_{e'}$. Due to very low counting rates for the backward angle kinematics, it was only possible to perform a single set of measurements at 260 MeV/c recoil momentum. The lever arm in ϵ between the forward and the backward kinematics, $\Delta\epsilon = 0.47$, is reasonably large and does not lead to excessive systematic errors.

It must be noted that $\mathbf{p}'$ and $\mathbf{q}$ cannot be perfectly aligned for all values of E_m simultaneously. We chose to have $\mathbf{p}'$ and $\mathbf{q}$ aligned at $E_m=25$ MeV. For other values of E_m, due to the misalignment, the cross section involves interference terms TT and TL. The TT contribution was calculated to represent at most 0.1% of the total cross section and could be neglected. The TL contribution is not negligible but it can be determined if additional measurements are performed with a $\mathbf{p}'$-$\mathbf{q}$ misalignment opposite to that of the original kinematics. An exact separation of TL in each bin in E_m would have required an additional measurement for each bin. This could not be done in our allotted time. However, we did perform a single supplementary measurement (kinematics S) at forward angle. We used this to achieve an approximate determination of the TL function, allowing us to correct for our misaligned kinematics. The three sets of kinematics (F, B, and S) are tabulated in Table I.

TABLE I. The three kinematics of the experiment. All energies and momenta are in MeV.

	E_e	$E_{e'}$	$\theta_{e'}$	$\theta_{p'}$	p'	p_r	E_m
F	670	419	34	36	657	260	25
B	396	146	80.4	21	657	260	25
S	670	432	34.8	43.5	640	245	25

The experimental setup is identical to that of Ref. [9]. Note, however, that a slot was dug in the proton spectrometer to reduce the minimal angle from 25° to 21°. This reduction improved the lever arm, $\Delta\epsilon$, from 0.35 to 0.47. As was done in [9], we introduced a small amount (0.5%) of hydrogen to the target in order to check the recoil momentum reconstruction. The accuracy was found to be better than 0.5 MeV/c. Such an error in p_r contributes less than 1.5% to the measured $^3\mathrm{He}(e,e'p)X$ cross sections. For the forward kinematics the average beam current was limited to 5 μA due to the low ratio of true to random coincidences (1.5 in the $2bbu$ but 0.23 in the continuum). For the backward angle the only limitation was the 14 μA current that the target could tolerate.

The data analysis generally followed that of [9]. Since the separation between the $2bbu$ and the continuum threshold is only 2.2 MeV for ^{3}He, the $2bbu$ event yield was integrated only up to $+2.0$ MeV in missing energy. In this condition the error on the cross section due to smearing between the $2bbu$ and the continuum is less than 1%. The continuum was deconvoluted for radiative effects as in [1]. The deconvolution was, however, much easier because for the present kinematics there is hardly any correlation between the recoil momentum and the missing energy, and the radiative tails are small.

In addition to the systematic errors quoted in [9] there is a contribution due to the uncertainty in the curvature of the spectral function in the acceptance, since its knowledge is required for the Monte Carlo simulation. Moreover, since kinematics F and S do not provide an exact determination of the TL contribution, we conservatively estimated that TL is known with a 20% systematic uncertainty which we propagated in the separation.

Figure 2 presents S_T^{expt} and S_L^{expt} in the continuum channel, $^3\mathrm{He}(e,e'p)pn$, together with theoretical predictions from a microscopic calculation [8]. The experimental values can be found in Table II. In this experiment, with a moderate p_r, we observe no peak in the continuum spectra. This was also the case in [1,2] at the same p_r. We notice in Fig. 2 a very large violation of the PWIA, since S_T^{expt} is much larger than

[1]The additional factor k, present in [9], appears only for the $2bbu$ channel.

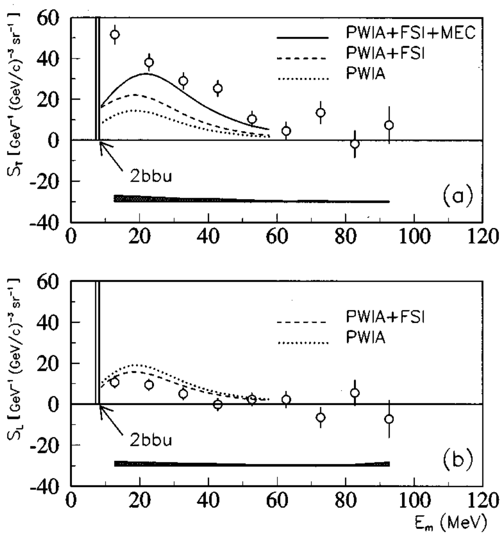

FIG. 2. Longitudinal (a) and transverse (b) experimental spectral functions in the continuum channel, ^{3}He$(e,e'p)pn$. The error bars are statistical only. The size of the systematic errors is indicated by the shaded area. The curves represent microscopic calculations [8] using a Faddeev wave function [11] with the RSC potential. The position of the $2bbu$ channel, ^{3}He$(e,e'p)^2$H, is indicated by a vertical band.

$S_L^{\rm expt}$. The theoretical curves are generated, similarly to $S_T^{\rm expt}$ and $S_L^{\rm expt}$, by dividing the theoretical nuclear cross sections by the cross sections on the off shell proton [10]. Three calculations are shown: PWIA, PWIA + FSI, and in the transverse case PWIA + FSI + MEC, where FSI's represent the final state interactions. No MEC contribution exists in the longitudinal cross section. In PWIA S_L and S_T are the same, the prediction is larger than $S_L^{\rm expt}$ and much smaller than $S_T^{\rm expt}$. The inclusion of FSI's and MEC's explains only part of the difference between $S_L^{\rm expt}$ and $S_T^{\rm expt}$

The integration of the experimental spectral functions over E_m leads to $\int S_L^{\rm expt} dE_m = 0.27 \pm 0.07 \pm 0.08$ and $\int S_T^{\rm expt} dE_m = 1.54 \pm 0.09 \pm 0.09$, where the first error is statistical and the second systematic and the unit is $({\rm GeV}/c)^{-3}$. The integral of $S_T^{\rm expt}$ is larger than that of $S_L^{\rm expt}$ by nearly eight standard deviations (statistical plus systematic) and the ratio is more than a factor of 5. The theoretical predictions, when all corrections are included (FSI's and MEC's), are $\int S_L^{\rm expt} dE_m = 0.42$ and $\int S_T^{\rm expt} dE_m = 0.98$. The longitudinal is only 1.3 standard deviations away but the transverse is 4.4. The calculation uses as input a ^{3}He wave function [11] obtained by solving the Faddeev equations for the RSC potential [12]. If instead a variational wave function [13] with the Argonne potential [14] is used, the results become $\int S_L^{\rm expt} dE_m = 0.59$ and $\int S_T^{\rm expt} dE_m = 1.37$. The calculation overestimates the longitudinal contribution by three standard deviations and is compatible with the data for the transverse contribution. These numbers show that it is impossible to conclude whether the problem is that the calculation overestimates the longitudinal contribution, underestimates the transverse one, or both.

In considering the *ratio* of the integrated longitudinal to the integrated transverse spectral functions, some of the experimental systematic errors and the theoretical uncertainty due to the choice of the wave function cancel out. FSI's and MEC's reduce the theoretical prediction for the ratio from unity (PWIA) to 0.43, regardless of which wave function is used. This is still much larger than the experimental ratio of $0.175 \pm 0.046 \pm 0.049$. The difference is 3.8 standard deviations (statistical plus systematic).

However the calculations should be treated cautiously because of the following inconsistency. The continuum spectral function can be obtained directly from the Faddeev ^{3}He wave function by taking its overlap integral with that of a neutron-proton pair together with a free proton. When the PWIA calculation, using the Faddeev wave function as input, is divided by the off-shell electron-proton cross section does not reproduce the above continuum spectral function as it should. The agreement is good for $E_m > 30$ MeV, but at low E_m the PWIA calculation predicts that the spectral function decreases when approaching the continuum threshold at $E_m = 7.7$ MeV (see the dotted curve in Fig. 2), whereas the spectral function obtained directly from the Faddeev wave function shows a strong increase.

TABLE II. Experimental transverse and longitudinal spectral functions in the continuum channel, ^{3}He$(e,e'p)pn$. The first error is statistical; the second systematic.

E_m MeV	p_r MeV/c	$S_T^{\rm expt}$ GeV^{-1}(GeV/c)$^{-3}$	$S_L^{\rm expt}$ GeV^{-1}(GeV/c)$^{-3}$
12.7	264	$51.6 \pm 4.7 \pm 3.1$	$10.7 \pm 2.9 \pm 1.9$
22.7	261	$38.1 \pm 4.3 \pm 2.3$	$9.4 \pm 2.9 \pm 1.5$
32.7	257	$29.0 \pm 4.2 \pm 1.6$	$5.0 \pm 3.0 \pm 1.1$
42.7	255	$25.3 \pm 4.0 \pm 1.4$	$-0.2 \pm 3.1 \pm 0.91$
52.7	252	$10.3 \pm 3.9 \pm 0.75$	$2.2 \pm 3.3 \pm 0.52$
62.7	250	$4.6 \pm 4.5 \pm 0.36$	$2.2 \pm 4.0 \pm 0.52$
72.7	248	$13.5 \pm 5.6 \pm 0.59$	$-6.5 \pm 5.0 \pm 0.51$
82.7	246	$-1.8 \pm 6.7 \pm 0.10$	$5.5 \pm 6.3 \pm 0.58$
92.7	245	$7.4 \pm 9.2 \pm 0.26$	$-7.2 \pm 9.2 \pm 1.7$

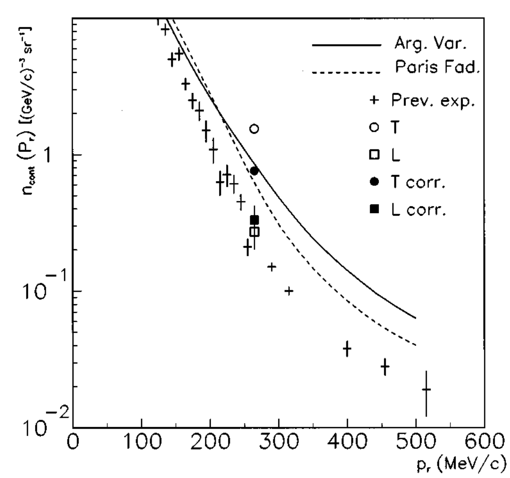

FIG. 3. Momentum distribution in the continuum channel, ^{3}He $(e,e'p)pn$. The data from previous experiments [2,15], which do not involve a T/L separation, are corrected for FSI's and MEC's, The data from the present experiment are presented both with and without corrections.

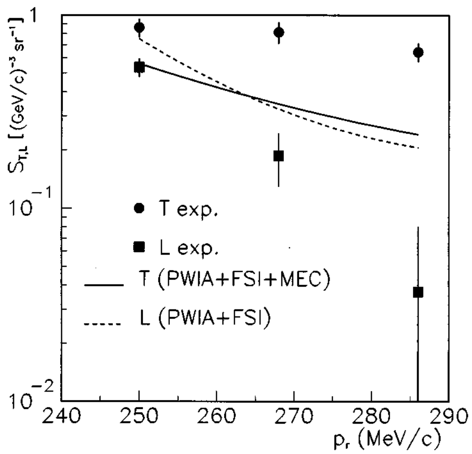

FIG. 4. Longitudinal and transverse experimental spectral functions in the $2bbu$ channel, ^{3}He$(e,e'p)^2$H. The curves are from microscopic calculations [8] using a Faddeev wave function [11] with the RSC potential.

The data can be used to extract the momentum distribution for the continuum channel, if we apply corrections for FSI's and MEC's:

$$n(p_r)=\int S^{\mathrm{expt}}(E_m,p_r)dE_m\times\frac{\sigma^{\mathrm{PWIA}}}{\sigma^{\mathrm{PWIA+FSI+MEC}}}. \qquad (2)$$

Figure 3 shows the momentum distributions extracted from the transverse and longitudinal experimental data together with results from previous experiments (without T/L separations) [2,15]. The results of our experiment are presented both before and after corrections, whereas the earlier data are only shown corrected. The momentum distribution determined from the longitudinal data is not very sensitive to the corrections and is compatible with earlier data taken at $\theta_{e'}=25^{\circ}$ where the cross section is dominated by the longitudinal contribution. The momentum distribution value at 260 MeV/c obtained from the transverse data remains much higher even after a large correction.

TABLE III. Experimental transverse and longitudinal spectral functions in the $2bbu$ channel, ^{3}He$(e,e'p)^2$H. The first error is statistical and the second one systematic.

p_r MeV/c	S_T^{expt} (GeV/c)$^{-3}$	S_L^{expt} (GeV/c)$^{-3}$
250	$0.860\pm0.092\pm0.064$	$0.535\pm0.058\pm0.048$
268	$0.815\pm0.104\pm0.049$	$0.187\pm0.057\pm0.031$
286	$0.643\pm0.072\pm0.035$	$0.037\pm0.043\pm0.019$

The data in the $2bbu$ channel, ^{3}He$(e,e'p)^2$H, have been sorted into three bins of p_r, and a T/L separation was performed in each bin. The resulting $2bbu$ experimental spectral functions are presented in Fig. 4 and tabulated in Table III. Similar conclusions hold as for the continuum channel: S_T^{expt} is much larger than S_L^{expt}, and the calculation cannot reproduce both at the same time. S_T^{expt} is better reproduced with the Argonne variational wave function and S_L^{expt} with the RSC Faddeev wave function. The slope of S_L^{expt} versus p_r is larger than the slope of S_T^{expt}; such a trend is seen in the calculations but the difference is smaller. Note, however, that this effect corresponds to three statistical standard deviations and that the systematic errors are of the same size.

We have performed a T/L separation of the ^{3}He$(e,e'p)pn$ cross section. We observe that S_L^{expt} is much smaller than S_T^{expt}, this effect cannot be explained by a microscopic calculation. The study of high proton momenta will have to be pursued out of the dip region, in the quasielastic region, which requires higher electron energy.

We would like to thank Jean-Marc Laget for his contribution to the execution and analysis of this work. The work of M.K.B. was supported in part by the U.S. National Science Foundation.

[1] J. M. Le Goff *et al.*, Phys. Rev. C **50**, 2278 (1994).
[2] C. Marchand *et al.*, Phys. Rev. Lett. **60**, 1703 (1988).
[3] S. Frullani and J. Mougey, Adv. Nucl. Phys. **14**, 1 (1984).
[4] K. Gottfried, Ann. Phys. (N.Y.) **21**, 29 (1963).
[5] L. Frankfurt and M. Strikman, Phys. Rep. **76**, 236 (1981).
[6] J. M. Laget, Nucl. Phys. **A358**, 275 (1981).
[7] J. M. Le Goff, Ph.D. thesis, Université Paris Sud, 1991, p. 43.
[8] J. M. Laget, in *New Vistas in Electronuclear Physics*, edited by Tomusiak *et al.* (Plenum, New York, 1986) p. 361.
[9] J. E. Ducret *et al.*, Nucl. Phys. **A556**, 373 (1993).
[10] T. De Forest, Jr., Nucl. Phys. **A392**, 232 (1983).
[11] Ch. Hadjuck and P. U. Sauer, Nucl. Phys. **A369**, 321 (1981).
[12] R. V. Reid, Ann. Phys. (N.Y.) **50**, 411 (1968).
[13] R. Schiavilla, V. R. Pandharipande, and R. B. Wiringa, Nucl. Phys. **A449**, 219 (1986).
[14] R. B. Wiringa, R. A. Smith, and T. L. Ainsworth, Phys. Rev. C **29**, 1207 (1984).
[15] E. Jans *et al.*, Nucl. Phys. **A475**, 687 (1987).